Journal of Atmospheric and Terrestrial Physics, Vol. 47, No. 1-3, pp. 283-290, 1985.
Printed in Great Britain.

0021-9169/85 $3.00 + .00
Pergamon Press Ltd.

Lower thermosphere densities of N_2, O and Ar under high latitude winter conditions

P. H. G. DICKINSON
Rutherford Appleton Laboratory, Chilton, Oxfordshire, U.K.

U. VON ZAHN
Physical Institute, Bonn University, Bonn, F.R.G.

K. D. BAKER
Center for Atmospheric and Space Studies, Utah State University, Utah, U.S.A.

and

D. B. JENKINS
Physics Department, University College of Wales, Aberystwyth, U.K.

(*Received for publication* 29 *August* 1984)

1. INTRODUCTION

Measurements of the neutral thermosphere made during the Energy Budget Campaign (northern Scandinavia, Nov/Dec 1980) included determinations of N_2, O and Ar densities using rocket-borne experiments. In this paper these results are presented and discussed in the context of other thermospheric observations in the campaign and are compared with a model atmosphere (USSA, 1976).

Because of the lack of photochemical sensitivity of argon and molecular nitrogen, measurement of the ratio of their concentrations in the lower thermosphere has been extensively used as an indicator of the extent to which diffusive separation of atmospheric constituents has occurred. At the altitudes of interest typical time constants for diffusive separation of argon are about 6 days at 100 km and 1 day at 115 km. However, at arctic latitudes, particularly during geomagnetically disturbed conditions, horizontal wind velocities in the lower thermosphere can approach 100 m s^{-1}, while horizontal changes in temperature and composition may be significant over distances of some hundreds of kilometres. Thus the time taken to transport air horizontally to regions with significantly different composition is of the order of an hour. This is short compared with the time constant for (vertical) diffusive separation, at least below about 125 km. Thus at high latitudes the Ar/N_2 ratio is affected by horizontal and vertical winds, as well as molecular and eddy diffusion.

Atomic oxygen is produced throughout the mesosphere and thermosphere, mainly by photodissociation of O_2. Its concentration is also controlled by eddy diffusion loss down into the mesosphere, where its lifetime changes from weeks above 90 km to hours below 80 km. Above the maximum in [O] near 95 km the distribution with height tends towards diffusive equilibrium. Horizontal winds can influence the distribution, especially at high latitudes. However, the lack of photodissociation during polar winter leads to transpolar asymmetry in [O] and an influx of oxygen atoms from the summer hemisphere. This may cause departures from simple diffusive equilibrium distributions in the thermosphere (DICKINSON *et al.*, 1980).

The measurements presented in this paper show striking differences in thermospheric distributions of the neutral constituents under different geomagnetic conditions.

2. EXPERIMENTAL METHODS

The techniques used in this work to measure argon, nitrogen and atomic oxygen densities have been described in detail elsewhere (WIRTH and VON ZAHN, 1981; DICKINSON *et al.*, 1980, 1981). A summary is presented below.

2.1. *Argon and molecular nitrogen*

Rocket-borne mass spectrometers were used to measure the densities of argon and molecular nitrogen (WIRTH and VON ZAHN, 1981). The gas within the instrument was ionised using an electron beam in an ion

source. The ions were accelerated into an electrostatic deflector followed by a magnetic deflector to separate the masses. Argon and nitrogen ion currents were measured simultaneously by separate electrometer sensors.

The payloads (E4) were launched at the times shown in Table 1, on Nike-Apache rocket vehicles. An ion getter pump was used to evacuate the instrument before launch. At 64 s after launch (59 km nominal altitude) the payload was separated from the rocket motor. During the remainder of the ascent gas releases within the instrument provided calibration signals, and a titanium sublimation pump was used to restore the vacuum. Shortly before apogee (125 km nominal altitude) the ion source cover was removed to allow ambient gas into the instrument. A downward pointing attitude for the orifice permitted good gas collection efficiency during the descent. The instrument sensitivity was constant down to about 100 km (by which height the gas influx had raised the pressure in the instrument enough to cause some loss of sensitivity). The collection efficiency was a function of mass, relative velocity and angle of attack of the incoming gas. The results were corrected for these factors, although the limited accuracy of attitude reconstruction means that the attitude dependence may not have been completely removed.

The experiment provided argon and molecular nitrogen densities between 95 and 125 km with a spatial resolution of < 100 m. Furthermore, from these results height profiles of the temperature could be deduced.

2.2. *Atomic oxygen*

The concentration of ground state O (^{3}P) oxygen atoms [O] was measured using rocket-borne UV resonance lamps. Two types of payload (E5 and E10) were used, on Petrel II and Taurus-Orion rocket vehicles, respectively. On the E5 payloads measurements were made of resonance fluorescence and absorption using the OI ($^3P_j - {}^3S_1$) triplet at 130 mm (DICKINSON *et al.*, 1980). The experiment on the E10 payload measured resonance fluorescence alone, using a lamp emitting the same triplet (HOWLETT *et al.*, 1980). The flight details are included in Table 1.

The lamps for the E5 payloads were calibrated before flight by measuring absorption in known atomic oxygen concentrations in a laboratory flowing afterglow. The absorption measurements on the rocket were over a path length of 40 cm perpendicular to the rocket axis using a deployed mirror. The experiment provided absolute values for [O] at concentrations above about 10^{10} cm^{-3}. The resonance fluorescence was normalised to the absorption values using a smoothed conversion curve linearly extrapolated to low concentrations. This method can measure concentrations as low as 2×10^{-7} cm^{-3} with a height resolution of 0.5 km and a precision (standard deviation) of $\pm 100\%$. This limit may be adversely affected by background signals due to aurorae or airglow. Lower concentrations may be detectable with reduced height resolution.

For the experiment on E10 the resonance fluorescence signal was converted to absolute values of [O] using measured photon fluxes and efficiencies of the lamp, sensor and viewing geometry. Allowance was made for the non-linear response of the resonance fluorescence experiment at high values of [O].

The resonance lamps were modulated in intensity with a 50% on–off duty cycle at 200 Hz to allow the resonance fluorescence signal from ambient [O] to be differentiated from background due to airglow and auroral emissions at 130 nm. On E5 the signals were sampled at 800 Hz, giving two measurements with the lamp on and two with it off per modulation cycle. The lamp emitted a weak afterglow during the first sample with the lamp 'off'. This gave rise to weak resonance fluorescence signals which could be found by subtraction of the following sample, which contained background only. The afterglow fluorescence was normally a constant proportion (near 5%) of the fluorescence with the lamp on. For part of one flight the full fluorescence plus background signal was saturating the counter electronics (in an aurora), but the afterglow plus background was not doing so. It was then possible

Table 1. Flight details

		Payload type	E4	E10	E5
		Constituents measured	[Ar][N_2]	[O]	[O]
		Launch site	Andøya	Andøya	Kiruna
		Group	Bonn	Utah	RAL/UCW
Salvo	Date	Conditions	Launch times		
C	11 Nov. 80	Quiet	00:12:00		00:12:00
B	16 Nov. 80	Mod. disturbance	03:31:00	03:16:00	
A2	30 Nov. 80	Strong disturbance			23:45:30

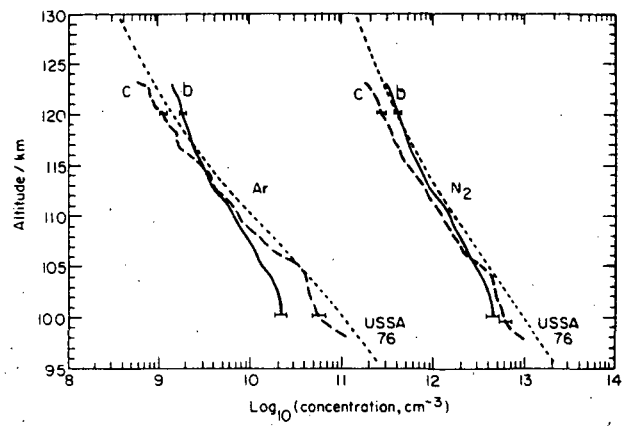

Fig. 1. Argon and nitrogen concentration (left and right, respectively). Measured by Bonn University Mass Spectrometers. b, Salvo B, moderately disturbed night; c, salvo C, quiet night; USSA 76, U.S. Standard Atmosphere. Flight details in Table 1. Uncertainties in the measured concentrations are ± 10% and ± 20% at 120 km and 100 km, respectively.

to use the afterglow data to fill in the lost data from the full fluorescence. A substantial part of the aurorally disturbed data was recovered in this way. The signals on the other two flights did not saturate.

From these measurements three atomic oxygen profiles have been derived. These are described in Section 3.2.

3. MEASUREMENTS

3.1. $[Ar]$, $[N_2]$ *and gas temperature results*

The mass spectrometer measurements of argon and nitrogen concentrations are shown in Fig. 1 for salvoes B and C. The error bars indicate the uncertainty in the absolute values of the concentrations ('accuracy'). The statistical errors ('precision') were too small to show. Also shown are the values given in the United States Standard Atmosphere (USSA, 1976) for the concentrations of these constituents.

In salvo C (curves c, Fig. 1) both constituents were close to 70% of the USSA 76 values over the height range of the measurements (100–125 km) except for perturbations below about 105 km, which may arise in part from imperfections in vehicle attitude reconstruction. The latter uncertainty is included in the error bars at 100 km.

By contrast, the results from salvo B (curves b, Fig. 1) show that the slope of the $[N_2]$ profile differed from USSA 76 in having greater scale heights and higher derived gas temperatures. An even greater departure from the USSA 76 occurred in the [Ar] profile.

The height variation of the concentration ratio $[Ar]/[N_2]$ is shown in Fig. 2 for salvoes B and C. Also shown are values derived from the USSA 76 and the upper and lower quartiles (labelled 3/4 and 1/4, respectively) of the range of earlier measurements by similar rocket-borne techniques [PHILBRICK *et al.*, 1974, 1978; TRINKS *et al.*, 1978; KENESHEA *et al.*, 1979; OFFERMANN *et al.*, 1981 (review)]. Thus at each height

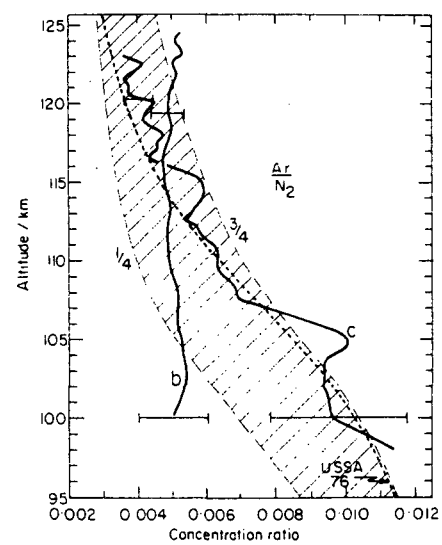

Fig. 2. Argon/nitrogen concentration ratios. b, Salvo B; c, salvo C; USSA 76, U.S. Standard Atmosphere. Shaded area includes 2nd and 3rd quartiles of earlier measurements (see text). Uncertainties in the measured ratios are ± 10% and ± 20% at 120 km and 100 km, respectively.

half of the earlier measurements lay in the shaded area of Fig. 2. The figure also shows the uncertainty in the measured ratios. This is no greater than the uncertainty in the individual concentrations, since some causes of error affect [Ar] and [N_2] similarly.

For salvo C (curve c, Fig. 2) the basic variation of the ratio with height is close to the USSA 76 and conforms with earlier measurements. However, the ratio [Ar]/[N_2] for salvo B (curve b, Fig. 2) was virtually independent of height over the height range of the measurements. This is a substantial departure from the expected behaviour. In particular it exceeds the upper quartile above 120 km yet falls below the lower quartile below 105 km. In contrast, earlier results broadly resembled the USSA 76 in height dependence, with the flight to flight variability being attributable largely to displacement of the curve in height (i.e. changes in the height of the turbopause). So although the salvo B profile spans the range of earlier results and is unexceptional at any given height, its height variation is much smaller than has been observed before.

The gas temperatures shown in Fig. 3 were deduced from the [N_2] profiles by integration downward along the profile, assuming hydrostatic equilibrium and an initial value for the gas temperature at 123 km on the profile. For each salvo the analysis was performed for three initial values of temperature. The dependence of the deduced temperatures upon the initial value is seen to diminish as the integration progresses downwards. The temperatures given in the USSA 76 are also shown. The salvo C results indicate temperatures in broad agreement with the USSA 76. The salvo B results suggest that there was a temperature enhancement of 40–60K at altitudes up to at least 118 km on that occasion.

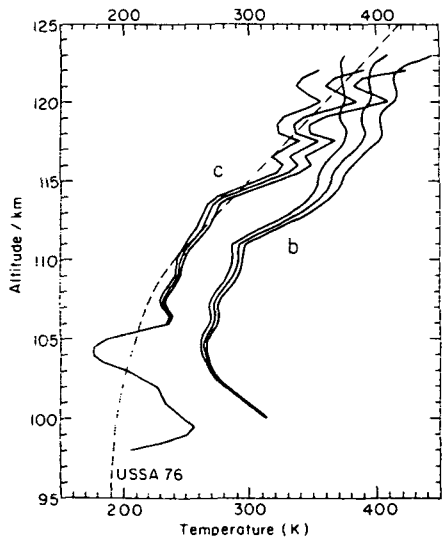

Fig. 3. Gas temperatures derived from nitrogen concentrations for three initial values at 123 km and assuming hydrostatic equilibrium. b, Salvo B; c, salvo C; USSA 76, U.S. Standard Atmosphere.

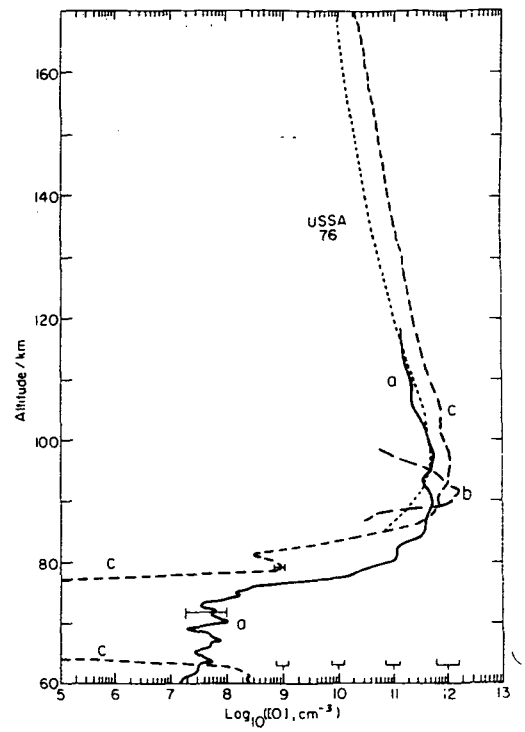

Fig. 4. Atomic oxygen concentrations for three nights. a, Salvo A2, very disturbed night; b, salvo B; c, salvo C. Measured by resonance fluorescence at 130 nm [Utah State University, (b)] and by resonance fluorescence and absorption [RAL/UCW (a, c)]. USSA 76, U.S. Standard Atmosphere. Statistical error bars shown on curves a and c. Absolute scale uncertainty shown above concentration axis.

3.2. [*O*] *results*

In Fig. 4 the three measurements of atomic oxygen are compared with the USSA 76 values. The standard deviations arising from random variations in the resonance fluorescence counts are indicated on the curves. At concentrations above about 10^{10} cm^{-3} these were too small to show. Uncertainty in the absolute scale is indicated above the concentration axis. This became greater at high concentrations due to the non-linear responses of the experiments. The results for the geomagnetically quiet day, salvo C (curve c), covered

the height range 60–170 km. Down to 120 km the concentrations were about 2.5 × USSA 76 values. The scale height was about 22 km, varying less with altitude than the USSA 76 values do. Some structure was evident below about 110 km and the local 'scale height' minima were about 10 km. At 96 km the peak concentration of atomic oxygen was 1.1×10^{12} cm^{-3}, as measured by the absorption experiment. Below a small layer with 10^9 cm^{-3} at 79 km the cut-off of the layer occurred at 77.5 km, to concentrations below 10^5 cm^{-3}. There was evidence of a region with [O] up to 10^8 cm^{-3} below 64 km from both ascent and descent data from the resonance fluorescence experiment.

For the moderately disturbed night, salvo B (curve b, Fig. 4), the atomic oxygen results cover the altitude range 86–98 km. At greater altitudes the high background signal due to aurorae and airglow raised the threshold for detection of resonance fluorescence signals. For that reason the absence of data above 98 km does not mean that no atomic oxygen was present. Thus the observed 'scale height' of 2 km near 95 km could have been due to local structure in the profile and should not be extrapolated to greater heights. The peak concentration deduced from the resonance fluorescence experiment was 1.4×10^{12} cm^{-3} at 92 km. The lowest concentration detected by this experiment was 3×10^{10} cm^{-3} at 86 km. This concentration was encountered at 84.5 km in salvo C and 79 km in salvo A2 (curve a), illustrating the flight to flight variability in the height below which the [O] layer cuts off. The topside result for salvo B is radically different from the other profiles, and indeed from previous measurements and models of atomic oxygen profiles. Possible causes within the experiment have been examined. In particular, the large background signals detected on this flight did not saturate the counter or cut off the resonance fluorescence signals. It is concluded that the results shown represent the actual [O] profile up to 98 km.

The results for the day with very disturbed geomagnetic conditions, salvo A2 (curve a), cover the altitude range from 60 to near 120 km (see Fig. 4). Intense auroral background emissions during this flight prevented measurements above 120 km due to saturation of the counting electronics. Above 95 km the [O] values straddle the USSA 76 and at 97 km a peak value of 5×10^{11} cm^{-3} was measured by the absorption experiment. At 90 km a second peak of similar concentration was observed, exceeding the USSA 76 by a factor of 2. Below 87 km the observed concentrations were greater than in salvo C and cut off 6 km lower. A weak concentration of 2×10^7–10^8 cm^{-3} was observed by the resonance fluorescence experiment between 76 and 60 km.

4. DISCUSSION

4.1. *Salvo C*

On the quiet day (salvo C) the atmospheric neutral constituents showed little departure from normal behaviour. The thermospheric temperatures deduced from the N_2 profile were close to the nominal USSA 76 values up to 115 km, above which they increased rather more slowly with height.

The atomic oxygen profile from salvo C shows a slightly larger scale height than is expected under diffusive equilibrium at 120 km. This is similar to earlier measurements in northern hemisphere winter (DICKINSON *et al.*, 1980) which are consistent with the assumption of a net downward flux of oxygen atoms at that time. Hence the larger scale heights should not be taken to indicate higher thermospheric temperatures than given by the USSA 76 or by the [N_2] scale heights during the same quiet day salvo. The structure in the atomic oxygen profile below 110 km was similar in the ascent and descent measurements and is therefore interpreted as normal horizontal stratification associated with atmospheric dynamics. One cause of this could be layered turbulence, giving rise to well mixed layers within which [O] 'scale heights' approach the total density scale height (e.g. 96–101 km, 88–91 km and 79–81 km). Another possible cause of the structure could be wind shears causing arrival of air masses at different heights from different locations and having different atomic oxygen contents determined by their respective photochemical histories. Structure might also arise from density/temperature fluctuations in gravity waves. The occurrence of similar structures at 100–115 km in [O], [N_2] and [Ar] is probably not significant, since the [O] measurement was at Kiruna and the others at Andøya. It is therefore difficult on this evidence alone to differentiate between the above mechanisms to account for the structure in [O].

4.2. *Salvo A2*

The atomic oxygen measurements (Fig. 4) show striking differences. Comparing the results from the quiet and very disturbed nights (curves c and a, respectively), the differences are as expected if a significant increase in eddy diffusion loss of oxygen atoms occurred on the disturbed night.

The reduced altitude of the atomic oxygen cut-off on the disturbed night means that there was a higher atom concentration in the region of rapid loss by three body recombination. The associated downward flux depleted the peak and topside of the layer and resulted in a change in total (column) content of oxygen atoms by a factor of two by comparison with the quiet night.

The enhanced concentrations at altitudes between 80 and 65 km on the disturbed night may be attributable to the production of oxygen atoms by high energy auroral particles dissociating O_2. The observed concentrations at these low altitudes are about 1% of the normal daytime values caused by solar photodissociation, but significantly higher than the minimum measureable concentration in the experiment (about 10^7 cm^{-3}).

4.3. *Salvo B*

On the geomagnetically moderately disturbed day (salvo B) the neutral constituents showed marked departures from normal behaviour. The thermospheric temperature deduced from the N_2 profile was 50 ± 10K higher than the USSA 76 at 110 km. As described in Section 3.1, the $[Ar]/[N_2]$ ratio was virtually constant throughout the height range observed (100–125 km), showing that on this occasion this part of the atmosphere was well mixed. The mixing ratio of 0.5% was less than half of the value in the lower atmosphere (1.2%). In addition, we note that the water vapor mixing ratio was comparatively high (about 10 ppm) and nearly constant throughout the altitude region 85–100 km (GROSSMANN *et al.*, 1985).

Mixing a standard atmosphere between 100 and 125 km would produce an Ar/N_2 mixing ratio of 0.84% and an increase in the upper bound of the mixed region cannot bring the ratio down below about 0.8%, as the mass of gas involved becomes small. Hence to produce the observed ratio of 0.5% requires net downward transport to displace the relatively argon-rich gas at lower altitudes. This downward transport was accompanied by a thorough mixing process, as indicated by the ratio Ar/N_2 being nearly constant over a 20 km altitude range. Both processes, downward bulk motion and large scale mixing, could well have been effected by a mesoscale meridional circulation cell including strong wind shears. Vigorous southward winds were measured above 100 km during salvo B at Kiruna by both an instrumented falling sphere experiment and a vapor release (REES *et al.*, 1985).

The southward component was more than 100 m s^{-1} at 120 km altitude and even stronger higher up. On the other hand, the data collected during the salvo B of the Energy Budget Campaign does not allow us to establish the details of this circulation pattern.

Zonally averaged models of thermospheric dynamics (e.g. ROBLE and KASTING, 1984) have limited spatial and temporal resolution and cannot be expected to provide a sufficiently detailed prediction of thermospheric behaviour for use as an input in analysing particular events such as are reported here, particularly when the measurements were taken in close proximity to the auroral oval.

The measurement of atomic oxygen at Andøya in salvo B (curve b, Fig. 4) is highly untypical. The large peak concentration and the layer bottom above the other measurements imply, by extension of the arguments used in Section 4.1 that there was little downward transport of atoms by eddy diffusion below the layer peak at 90 km. This is not inconsistent with the gross downward flux implied above from the Ar/N_2 results at higher altitudes for this night, since eddy diffusion transport requires no bulk movement and vice versa. The steep topside of the atomic oxygen layer is very difficult to explain. Bulk downward transport could not provide '[O] depleted' air, since the typical mixing ratio $[O]/[N_2]$ increases with altitude. It is possible that the effect is an extreme example of the local structuring normally seen in [O] profiles and that the distribution at greater altitudes was more typical, but not detected due to the intense auroral background emissions.

In view of the problem in interpreting the [O] profile from salvo B it is interesting to note some qualitative similarities between the observed atomic oxygen concentrations (Fig. 4) and the predictions of ROBLE and KASTING (1984) for 69°N (Fig. 5). They considered three cases: solar heating only; solar heating plus high latitude heating; solar heating plus three times as much high latitude heating. Profiles interpolated from their contour figures 3b, 5b and 7b are shown in this paper in Fig. 5, labelled C, A and B, respectively, to facilitate comparison with the observations in Fig. 4.

The points of similarity are as follows. Firstly, the moderate high latitude heating decreased the modelled concentration by about a factor of two from the layer peak upwards. It did not affect the scale height in the thermosphere. This is closely similar to the relationship between the measurements in salvoes C and A2. Secondly, the model with stronger heating predicted a severe depletion in the thermospheric concentration (a factor of 10 at 150 km in the model) associated with a marked reduction in thermospheric scale height by about a factor of 2 up to 150 km (Fig. 5, curve B). From this we may imply that dynamical/chemical effects can cause changes in the lower thermosphere which are qualitatively similar to the observations in salvo B (Fig. 4, curve b). The measured high latitude heating on that occasion did not exceed that seen during salvo A2 (BAUMJOHANN *et al.*, 1984). However, the location of the heat input was overhead for salvo B but somewhat further south for salvo A2, while the measurements were made later at night for salvo B (see Table 1). Such detailed differences on the two occasions may have resulted in differing locations for the boundary between the solar-driven and high latitude circulations. To the north of this boundary the vertical winds are upward

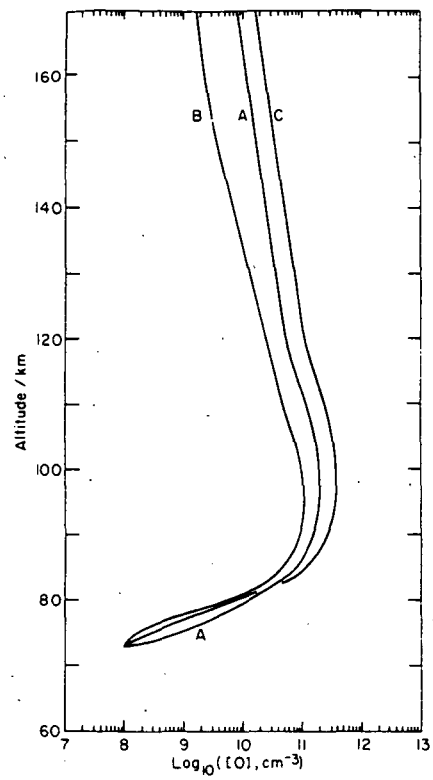

Fig. 5. Model profiles of atomic oxygen concentration for 69°N (winter) interpolated from zonally averaged chemical-dynamical model of ROBLE and Kasting (1984). C, solar heating only; A, solar and high latitude heating; B, solar and 3 × high latitude heating.

and to the south they are downward [the predicted location of this boundary, particularly below 150 km, depends upon what model is used (cf. ROBLE and KASTING, 1984; ROBLE *et al.*, 1977)]. For these reasons the points of similarity between the observations and the predictions of ROBLE and KASTING (1984) are not thought to contradict the conclusion from the argon depletion in salvo B that a downwind had been occurring on that occasion.

CONCLUSIONS

Measurements of neutral atmospheric constituents during the Energy Budget Campaign show that under quiet geomagnetic conditions there was reasonable agreement with the United States Standard Atmosphere (USSA 76). $[N_2]$ and [Ar] were about 70% of the predicted values and [O] about 2.5 times greater. During a night with moderate geomagnetic disturbance, and substantial accumulated Joule heating from auroral activity, there were striking departures from the USSA 76. These included a constant Ar/N_2 mixing ratio of 0.5% from 100 to 125 km. To explain this a downward bulk movement combined with large scale mixing in the thermosphere is invoked. Increased values of gas temperatures were derived from the N_2 profile and also an unusually narrow layer of atomic oxygen was detected.

On a more strongly disturbed night an atomic oxygen profile showed half the column content observed on the quiet night, lower peak concentration and increased concentration at lower altitudes. These effects are consistent with enhanced eddy diffusion loss during the auroral activity.

Acknowledgements—The authors are grateful to their respective institutions for support and to the staff of the Andøyà and Kiruna rocket ranges for their invaluable services.

REFERENCES

BAUMJOHANN W., GUSTAFSSON G., NIELSEN E., RANTA H. and EVANS D. S.	1985	*J. atmos. terr. Phys.* **47**, 27.
DICKINSON P. H. G., BAIN W. C., THOMAS L., WILLIAMS E. R., JENKINS D. B. and TWIDDY N. D.	1980	*Proc. R. Soc.* **A369**, 379.
DICKINSON P. H. G., WILLIAMS E. R. and JENKINS D. B.	1981	*Energy Budget Campaign 1980: Experiment summary*, OFFERMANN D. and THRANE E. V. EDS. p. 340. BMFT-FB-W-81-052, Bundesministerium für Forschung und Technologie, Bonn, F.R.G.
GROSSMANN K. U., FRINGS W. G., OFFERMANN D., ANDRÉ L., KOPP E. and KRANKOWSKY D.	1985	*J. atmos. terr. Phys.* **47**, 291.
HOWLETT L. C., BAKER K. D., MEGILL L. R., SHAW A. W., PENDLETON W. R. and ULWICK J. C.	1980	*J. geophys. Res.* **85**, 1291.
KENESHEA T. J., ZIMMERMAN S. P. and PHILBRICK C. R.	1979	*Planet. Space Sci.* **27**, 385.
OFFERMANN D., FRIEDRICH V., ROSS P. and VON ZAHN U.	1981	*Planet. Space Sci.* **29**, 747.

PHILBRICK C. R., GOLOMB D., ZIMMERMAN S. P., KENESHEA T. J., MCLEOD M., GOOD R. D., DANDEKAR B. S. and REINISCH B. W.	1974	*Space Res.* **14**, 89.
PHILBRICK C. R., SCHMIDLIN F. J., GROSSMANN K. U., LANGE G., OFFERMANN D., BAKER K. D., KRANKOWSKY D. and VON ZAHN U.	1985	*J. atmos. terr. Phys.* **47**, 159.
REES D., CHARLETON P., CARLSON M. and ROUNCE P.	1985	*J. atmos. terr. Phys.* **47**, 195.
ROBLE R. G., DICKINSON R. E. and RIDLEY E. C.	1977	*J. geophys. Res.* **82**, 5493.
ROBLE R. G. and KASTING J. F.	1984	*J. geophys. Res.* **89**, 1711.
TRINKS H., OFFERMANN D., VON ZAHN U. and STEINHAUER C.	1978	*J. geophys. Res.* **83**, 2169.
USSA	1976	*United States Standard Atmosphere*. U.S. Govt. Printing Office, Washington DC.
WIRTH J. and VON ZAHN U.	1981	*Energy Budget Campaign 1980: Experiment summary*, OFFERMANN D. and THRANE E. V. Eds, p. 310. BMFT-FB-W-81-052, Bundesministerium für Forschung und Technologie, Bonn, F.R.G.